04,16

Calculation from first principles of structure and properties of cubic phase α -KY₃F₁₀

© R.A. Evarestov, N.A. Bogachev, K.S. Prichisly

St. Petersburg State University,

St. Petersburg, Russia

E-mail: r.evarestov@spbu.ru

Received June 1, 2025 Revised June 10, 2025 Accepted June 10, 2025

Calculations were made from first principles for the structure and electronic properties of crystal KY_3F_{10} by the density functional method in the LCAO basis with geometry optimization. It was found that the use of the hybrid HSE06 functionality provides the best agreement with experimental data compared to other approaches. Analysis of dispersion curves of phonons confirmed the stability of crystal KY_3F_{10} structure in the cubic phase.

Keywords: KY₃F₁₀, rare earth elements, double fluorides, DFT, HSE06 LCAO, GGA PBESOL, POB-TZVP-REV2

DOI: 10.61011/PSS.2025.06.61688.152-25

1. Introduction

Double fluorides of alkali metals-rare earth elements and solid solutions produced by introduction of lanthanide ions into them as doping components, are the widely studied compounds in the fields of development of materials for photovoltaics, photocatalysis, bioimaging, luminescent thermometry, protection of securities, luminescent sensors etc. [1–12]. The advantage of using these compounds consists in their low toxicity, possibility to vary the composition of compounds in the wide range and combination of several functional properties in one material (for example, luminescent and magnetic ones), easy production of nanosize parties of target compounds by methods of green chemistry [13–19].

The key role among the principal properties of such compounds belongs to the nature of the matrix acting as a master for doped ions, and its crystalline structure. Currently the family of compounds based on sodiumyttrium fluoride matrix NaYF4 is the most popular object of the comprehensive study and, accordingly, the most studied one both from the theoretical and the practical sides [20–23]. Another promising compound among double fluorides is KY_3F_{10} [24], but it is necessary to note that the scope of studies for this compound and solid solutions on its basis is much less [19]. For an individual fluoride KY_3F_{10} we know structural and spectral data obtained experimentally from the study of single crystals.

It is known that the compound with composition KY_3F_{10} exists in four different crystalline phases — cubic α - KY_3F_{10} , β - KY_3F_{10} and δ - $KY_3F_{10} \cdot xH_2O$, and also tetragonal γ - KY_3F_{10} [25–27], and among the listed ones, the cubic one α - KY_3F_{10} (Fm-3m, N° 225) is crystallized under normal conditions, is the most thermodynamically stable and well-studied phase [26,28,29]. The study of single

crystals α -KY₃F₁₀ by Raman scattering spectroscopy and IR spectroscopy of reflection made it possible to identify IR and Raman-active phonons [30,31]. It is also reported that the width of the band gap α -KY₃F₁₀ has the order of $10\,\text{eV}$ [32]. It is necessary to note that the same value is attributed to the other, tetragonal phase [33].

Even though α -KY $_3$ F $_{10}$ has been an object of study for a long time, theoretical studies for this compound in the available literature are of fragmented nature [34,35]. In this article we cite the results of theoretical modeling of crystalline structure and vibration spectra of KY $_3$ F $_{10}$, performed by the density functional method in the LCAO basis from first principles with geometry optimization.

2. Calculation procedure

In this paper the non-empirical calculations of crystal KY_3F_{10} were carried out for its cubic phase with spatial group of symmetry 225 (Fm-3m). Crystalline lattice-cubic, face-centered, with two formula units (28 atoms) in a primitive lattice cell [36].

Figure 1 shows the structure of this crystal and marks the Wyckoff positions occupied by atoms. Ratios of Wyckoff positions occupied by atoms are specified for a cubic cell comprising four primitive cells. A primitive elementary cell contains two groups of atoms, which in the ion model form subsystems $[KY_3F_8]^{2+}$ and $[KY_3F_{12}]^{2-}$. In the first case the fluorine atoms are located in cube tops, in the second one — in the cube-octahedron tops. Such structure helps to create the admixture atoms of lanthanides that substitute the yttrium atom located in the center of polyhedrons that are formed by fluorine atoms. Crystals KY_3F_{10} activated by lanthanides are widely studied [19] thanks to their use in the modern nanomaterials.

Atoms	Experiment*, $a = 11.553 \text{ Å}$	РВЕ	PBESOL**, $a = 11.431 \text{Å}$	HSE06*** $a = 11.554 \text{Å}$
Y1 24e	0.24035 0 0	0.24035 0 0	0.24006 0 0	0.24042 0 0
K1 8c	0.25 (3)	0.25 (3)	0.25 (3)	0.25 (3)
F1 32f	0.11184 (3)	0.11230 (3)	0.11157(3)	0.11130 (3)
F2 48i	0.5 0.16574 (2)	0.5 0.16585 (2)	0.5 0.16623 (2)	0.5 0.16546 (2)

Table 1. Atom positions in crystal KY₃F₁₀. Cartesian coordinates of atoms are given in units x/a, y/a, z/a, where a is a parameter of a cubic lattice

Note: * [31], ** calculations with potential PBESOL in this paper, *** calculations with potential HSE06 in this paper.

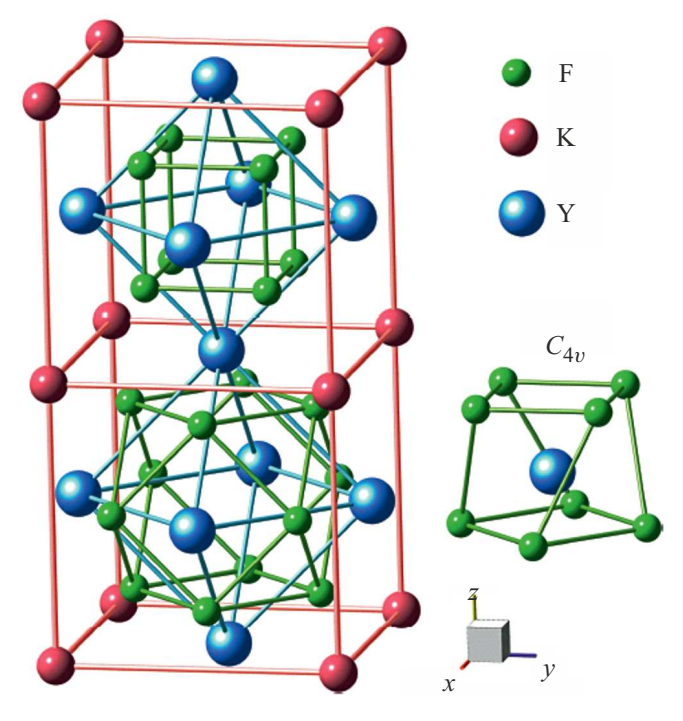


Figure 1. Atomic structure of crystal KY_3F_{10} (spatial group Fm-3m) with two formula units in a primitive cell (28 atoms): Y 24e, K 8c, F2 32f, F1 48i.

In this paper the calculations of the atomic, electronic structure and frequencies of atom vibrations in crystal KY_3F_{10} were carried out by density functional method with two exchange-correlation potentials: hybrid HSE06 and GGA PBESOL. CRYSTAL17 software [37] was used to calculate the crystalline solid bodies in the basis of atomic functions of Gaussian type.

For potassium and fluorine atoms an all-electron atomic basis POB-TZVP-REV2 was used [38]. For yttrium atoms, basis POB-TZVP-REV2 was used, obtained with relativistic pseudopotential for core electrons in [39], with valence electrons $4s^24p^65s^25p$ and polarizing functions of d and f type.

Summation over the Brillouin zone (BZ) was done using Monkhorst-Pack scheme [40] with $8\times8\times8$ k-points and precisions 8, 8, 8, 8, 16 for single-electron, Coulomb and exchange integrals. In other words, during direct-lattice summation, single-electron integrals and two-electron Coulomb integrals lower than 10^{-8} are estimated using a multipole expansion, and the two-electron exchange integrals lower than 10^{-16} are ignored. Self-agreement by electron density to solve single-electron equations was done with precision of up to $3\cdot10^{-9}\,\mathrm{eV}$. The parameter of the crystal lattice and coordinates of all atoms were optimized until the forces on the atoms exceeded $0.003\,\mathrm{eV/A}$.

To calculate the phonon frequencies, the following method was used. After finding the equilibrium geometry of the crystal, the frequencies of atom vibrations were calculated by the method for "frozen" phonons [41] in harmonic approximation. Internal values of the dynamic matrix (i. e. squared frequencies of phonons) were estimated numerically, adding small distortions of the crystal geometry. To build phonon dispersion curves, the method of the expanded lattice cell was used [42], which made it possible to calculate the frequencies of vibrations in the points of the Brillouin zone, which differ from point Γ (0,0,0).

To calculate the high-frequency dielectric constant of the crystal, the method of the perturbation theory was used to solve the electronic equation, if the electric field was present [43].

Non-empirical calculations of the structure and electron properties

Experimental study of the crystal KY_3F_{10} structure continues for more than 20 years. At the same time, non-empirical calculations of such structure are scarce and made both with using atomic potentials [44], and density functional theory [45].

In Table 1 we compare for the lattice constant and crystallographic coordinates of atoms the results of our PBESOL and HSE06 LCAO calculations for crystal KY_3F_{10} to the results found experimentally and in the flat wave

Bond	PBE***	PBESOL **	HSE06**	Experiment *
Y-Y	3.917	3.881	3.928	3.914
Y-K	4.082	4.043	4.086	4.078
Y-F1	2.196	2.181	2.199	2.200
Y-F2	2.330	2.326	2.350	2.349
K-F2	2.836	2.741	2.776	2.755
K-F1	3.203	3.162	3.202	3.193
F2-F2	2.495	2.551	2.572	2.586
F1-F1	2.688	2.708	2.703	2.706
F1-F1	2.784	2.741	2.763	2.743
F1-F2	2.976	2.973	2.910	2.935

Table 2. Interatomic distances (in Å) in crystal KY₃F₁₀

Note: * [31]; ** Calculations in this paper; *** [45].

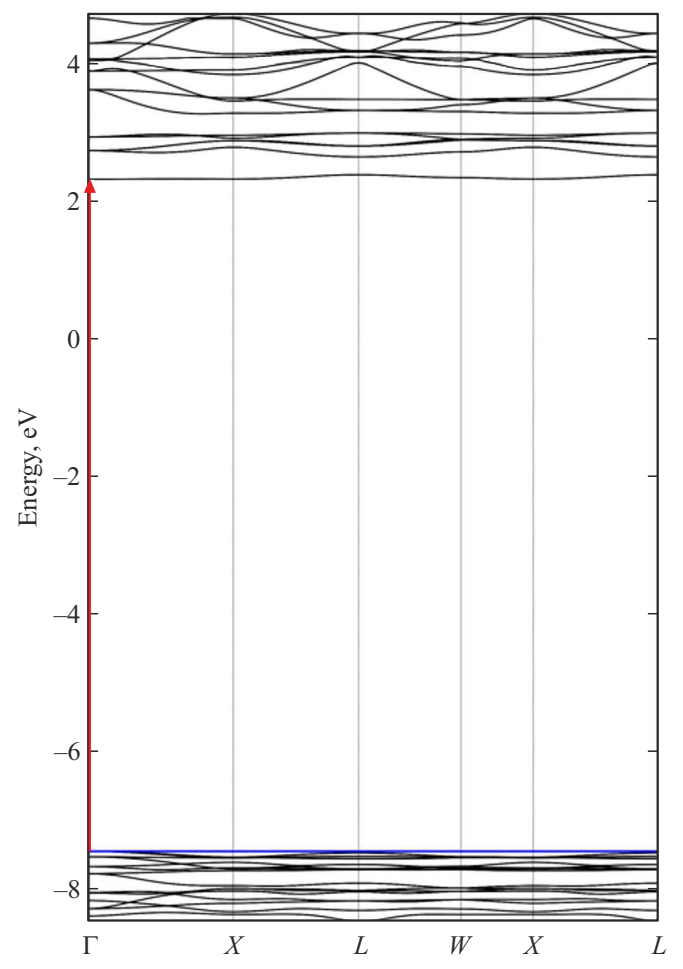


Figure 2. Electron zones for crystal KY_3F_{10} . Calculation of HSE06.

calculations using DFT PBE method [45]. You can see that the difference between the results of calculations in the atomic and flat wave bases is low (does not exceed 0.0077 in the fractions of the lattice constant). However, the best agreement between the theory and the experiment is provided by the calculations with the hybrid HSE06 potential.

In Table 2 the same comparison is provided for interatomic distances (bond lengths). Conclusions made using data of Table 1 are practically the same as the conclusions on the basis of the analysis of interatomic distance calculation results. In particular, the maximum difference of the interatomic distance calculated using HSE06 method from the experimental one is small, and for F1-F2 bond it is 0.025 Å. For the same bond such difference in PBESOL calculations is 0.041 Å and 0.038 Å for a flat wave and a LCAO calculations, accordingly.

Figure 2 presents the zonal electron structure of crystal KY_3F_{10} . The top of the valence band and the bottom of the conduction band are in point Γ (0,0,0) i.e. the interband transition is direct. The top valence band is formed, mainly, with 2p states of the fluorine atoms. For the band gap width the values that we calculated were equal to $10.50\,\mathrm{eV}$ (PBESOL) and $9.73\,\mathrm{eV}$ (HSE06). These values agree with data from [33], where for the width of the band gap it is specified that it is $> 10\,\mathrm{eV}$. At this time there is no reliable experimental data on the width of the band gap, as well as non-empirical calculations for this crystal with geometry optimization. In this paper such calculations have been done for the first time.

For the refractive index, we obtained values 1.46 (PBESOL) and 1.45 (HSE06), which is close to the experimental value 1.47 [48]. The theoretical value of high-frequency dielectric constant of 2.10 that we calculated is close to value 2.30, found in [31].

Vibration	*	PBESOL**	HSE06 **	Experiment *
A_{1g}	263	283	275	273
A_{1g}	321	319	321	318
A_{1g}	359	355	356	355
E_{g}	150	144	143	142
E_{g}	229	232	230	225
E_{g}	368	388	378	376
E_{g}	492	511	501	495
T_{2g}	89	99	98	92
T_{2g}	171	164	165	167
T_{2g}	246	187	184	_
T_{2g}	282	279	289	_
T_{2g}	326	338	329	324
T_{2g}	365	375	371	363
T_{1u}	111	103	104	102
T_{1u}	170	180	184	174
T_{1u}	237	243	239	238
T_{1u}	263	259	263	259
T_{1u}	308	311	306	298
T_{1u}	362	357	350	353
T_{1u}	501	506	495	501

Table 3. Frequencies of normal vibrations (cm⁻¹)

Note: * [45]; ** This paper.

4. Calculation of vibration frequencies in IR and RS spectra

Important information on optical properties of crystalline solid bodies is obtained when the Raman scattering (RS) and infrared absorption (IR) spectra are studied. interpretation of such spectra, based on the calculations in harmonic approximation, it is essential to use the point group of crystalline class, the irreducible representations of which are used to classify the atom vibrations in the crystal. For crystal KY₃F₁₀ such group is Oh cubic group. [46] contains the symmetry of phonons in crystal KY₃F₁₀. The Raman spectrum contains 13 frequencies $(3A_{1g} + 4E_g + 6T_{1g})$, and the IR spectrum — 7 frequencies with symmetry T_{1u} . The same paper attempted to calculate the frequencies of vibrations in crystal KY₃F₁₀ based on the model that contains 4 adjustment parameters and using experimental data from IR spectra of crystal KY₃F₁₀.

To calculate force constants, [31] used experimental values of bond lengths in crystal KY_3F_{10} . Therefore, the results

obtained in this paper are half-empirical. Non-empirical calculations by density functional method PBESOL on a flat wave basis were carried out by A. Togo [47]. Besides, Phonopy [48] software is used, and cyclical model of the crystal obtained by expansion of a primitive lattice cell. Dispersion curves were built for phonons, and the absence of the imaginary phonon frequencies for crystal KY_3F_{10} was found, i.e. the absence of the possible phase transition with the symmetry was confirmed. Densities of phonon states and thermodynamic properties at constant volume. However, the calculation is not in fact from first principles, since it uses experimental data for the crystal structure. Besides, no comparison is done for the obtained frequencies of vibrations with the experimental data on IR and RS spectra.

This paper for the first time performs in series the theoretical PBESOL and HSE06 calculations of phonon dispersion in crystal KY_3F_{10} with optimization of the structure geometry. Besides, the calculated frequencies of vibrations are also compared to the data of experiment on IR and RS spectra.

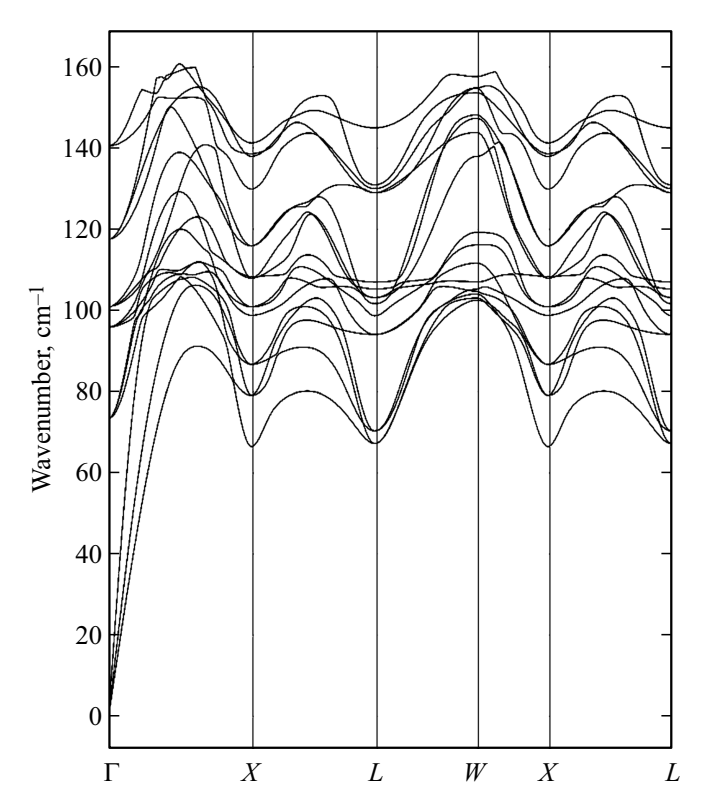


Figure 3. Phonon dispersion in crystal KY_3F_{10} .

From Figure 3 it follows that in the calculation from first principles there are no imaginary frequencies in the phonon spectrum, which confirms the stability of the considered structure and agrees with the data of calculations [45] with PBE functionality that were carried out for experimental geometry.

From Table 3 you can see that the agreement with the experiment for vibration frequencies in process of the calculation from first principles improves in transition from PBESOL functionality to hybrid HSE06 functionality.

5. Conclusion

The calculations from first principles with geometry optimization that were first carried out by the method of density functional in the LCAO basis result in the best agreement with the experiment for the structure and electron properties of crystal KY₃F₁₀ when selecting the hybrid functionality HSE06. Flat wave calculations with such functionality are considerably more labor-intensive compared to those in the LCAO basis. Based on the analysis of the calculated curves of phonon dispersion, no imaginary frequencies were detected, which confirms the stability of the calculated structure, i.e. absence of phase transitions in cubic modification of crystal KY₃F₁₀ with spatial group Fm-3m (225). Agreement with the experiment for frequencies of phonons in IR and RS spectra improves

in transition from PBESOL functionality to hybrid HSE06 functionality.

Conflict of interest

The authors declare no conflict of interest.

Acknowledgments

The study was performed using the equipment provided by the resource center of the Saint Petersburg State University Research Park "Computing Center of Saint Petersburg State University".

Funding

The study was supported by grant from the Russian Science Foundation No. 24-73-00034(https://rscf.ru/project/24-73-00034/ data is available as of June 1, 2025).

References

- T.P. van Swieten, D. Yu, T. Yu, S.J.W. Vonk, M. Suta,
 Q. Zhang, A. Meijerink, F.T. Rabouw. Adv. Opt. Mater. 9,
 1, 2001518 (2021).
- [2] A. Ćirić, S. Stojadinović, M.D. Dramićanin. Ceram. Int. 46, 14, 23223 (2020).
- [3] D. Pominova, V. Proydakova, I. Romanishkin, A. Ryabova, S. Kuznetsov, O. Uvarov, P. Fedorov, V. Loschenov. Nanomaterials. 10, 10, 1992 (2020).
- [4] M. Tou, Y. Mei, S. Bai, Z. Luo, Y. Zhang, Z. Li. Nanoscale. 8, 1, 553 (2016).
- [5] J. Hu, R. Wang, R. Fan, Z. Huang, Y. Liu, G. Guo, H. Fu. J. Lumin. 217, 1, 116812 (2020).
- [6] T.F. Schulze, T.W. Schmidt. Energy Environ. Sci. **8**, *1*, 103
- [7] W. Liu, W. Zhang, R. Liu, G. Li New. J. Chem. 45, 22, 9818 (2021).
- [8] D.T. Klier, M.U. Kumke. J. Phys. Chem. C **119**, *6*, 3363 (2015).
- [9] E. Lu, J. Pichaandi, L.P. Arnett, L. Tong, M.A. Winnik. J. Phys. Chem. C 121, 33, 18178 (2017).
- [10] T.K. Hill. A.M. Mohs. WIREs Nanomed. Nanobiotechnol. 8, 4, 498 (2016).
- [11] J.-X. Sun, J.-Z. Xu, Y. An, S.-Y. Ma, C.-Q. Liu, S.-H. Zhang, Y. Luan, S.-G. Wang, Q.-D. Xia. J. Control. Release. 353, 1, 832 (2023).
- [12] X. Chen, Z. Zhao, M. Jiang, D. Que, S. Shi, N. Zheng. New J. Chem. 37, 6, 1782 (2013).
- [13] C. Sassoye, G. Patriarche, M. Mortier. Opt Mater (Amst). 31, 8, 1177 (2009).
- [14] A. Paściak, M. Misiak, K. Trejgis, K. Elżbieciak-Piecka, O. Bezkrovnyi, Ł. Marciniak, A. Bednarkiewicz. J. Alloys Compd. 934, 1, 167900 (2023).
- [15] A.A. Dovzhenko, A.A. Betina, T.S. Bulatova, N.A. Bogachev, V.G. Nikiforov, A.D. Voloshina, R.R. Zairov, A.R. Mustafina, A.S. Mereshchenko, B.S. Akhmadeev Mendeleev Commun. 34, 5, 637 (2024).

- [16] T.S. Bulatova, N.A. Bogachev, A.A. Betina, A.N. Smirnov, E.V. Solovieva, M.Yu. Skripkin, A.S. Mereshchenko. Russ. J. Gen. Chem. 92, 12, 2845 (2022).
- [17] P.P. Fedorov, A.A. Luginina, S.V. Kuznetsov, V.V. Osiko. J. Fluor Chem. 132, 12, 1012 (2011).
- [18] S. Kedar, R. Sudhir, M.I. Ahmad, M. Kumar. J. Lumin. 228, 1, 117654 (2020).
- [19] C. Cressoni, F. Vurro, E. Milan, M. Muccilli, F. Mazzer, M. Gerosa, F. Boschi, A. Spinelli, D. Badocco, P. Pastpre, N. Delgado, M. Collado, P. Marzola, A. Speghini. ACS Appl. Mater. Interfaces 15, 9, 12171 (2023).
- [20] G. Yao, M.T. Berry, P.S. May, D.S. Kilin. Int. J. Quantum Chem. 112, 24, 3889 (2012).
- [21] G. Yao, M.T. Berry, P.S. May, D. Kilin, J. Phys. Chem. C 117, 33, 17177 (2013).
- [22] B. Jiang, X. Wang. J. Alloys Compd. 831, 1, 154785 (2020).
- [23] D. Kumar, K. Verma, S. Verma, B. Chaudhary, S. Som, V. Sharma, V. Kumar, H.C. Swart. Physica B Condens. Matter 535, 1, 278 (2018).
- [24] P. Serna-Gallén. Crystals (Basel) 14, 9, 762 (2024).
- [25] P. Serna-Gallén, H. Beltrán-Mir, E. Cordoncillo, R. Balda, J. Fernández. J. Alloys Compd. 953, 1, 170020 (2023).
- [26] A. Grzechnik, W.A. Crichton, J.-Y. Gesland. Solid State Sci. 5, 5, 757 (2003).
- [27] C. Cao, H.K. Yang, B.K. Moon, B.C. Choi, J.H. Jeong, K.H. Kim. J. Mater. Res. 27, 23, 2988 (2012).
- [28] E.P. Chukalina, T.A. Igolkina, D.N. Karimov. Opt. Spectrosc. 130, 1, 69 (2022).
- [29] D.N. Karimov, I.I. Buchinskaya, N.A. Arkharova, A.G. Ivanova, A.G. Savelyev, N.I. Sorokin, P.A. Popov. Crystals (Basel) 11, 3, 285 (2021).
- [30] M. Mortier, J.Y. Gesland, M. Rousseau, M.A. Pimenta, L.O. Ladeira, J.C.M. Da Silva, G.A. Barbosa. J. Raman Spectrosc. 22, 7, 393 (1991).
- [31] E.N. Silva, A.P. Ayala, J.-Y. Gesland, R.L. Moreira. Vib. Spectrosc. 37, 1, 21 (2005).
- [32] L. Guillemot, P. Loiko, R. Soulard, A. Braud, J.-L. Doualan, A. Hideur, P. Camy. Opt. Express 28, 3, 3451 (2020).
- [33] N.G. Debelo, F.B. Dejene, K.T. Roro. Mater. Chem. Phys. 190, 1, 62 (2017).
- [34] J. Dabachi, M. Body, J. Dittmer, A. Rakhmatullin, F. Fayon, C. Legein. Dalton Transactions. **48**, *2*, 587 (2019).
- [35] R.A. Jackson, E.M. Maddock, M.E.G. Valerio. IOP Conf. Ser. Mater. Sci. Eng. 15, 1, 1012014 (2010).
- [36] A. Grzechnik, J. Nuss, K. Friese, J.-Y, Gesland, M. Jansen, Z. Kristallogr. 217, 460 (2002)
- [37] A. Dovesi, V.R. Saunders, C. Roetti, R. Orlando, C.M. Zicovich-Wilson, F. Pascale, B. Civalleri, K. Doll, N.M. Harrison, I.J. Bush, P. D'Arco, M. Llunell, M. Caus'a, Y. Noël L. Maschio, A. Erba, M. Rerat, S. Casassa. CRYSTAL17 User's Manual, University of Turin, Torino, Italy (2018).
- [38] D. Vilela Oliveira, M.F. Peintinger, J. Laun, T. Bredow. J. Comput. Chem. **40**, 2364 (2019).
- [39] J. Laun, T. Bredow. J. Comput. Chem. 43, 839 (2022).
- [40] H.J. Monkhorst, J.D. Pack. Phys. Rev. B 13, 5188 (1976).
- [41] M. Ferrero, M. Rérat, B. Kirtman, R. Dovesi. J. Chem. Phys. 129, 244110 (2008).
- [42] R.A. Evarestov, A.V. Bandura. Theor. Chem. Accounts, 137, 14 (2018).
- [43] M. Ferrero, M. Rérat, R. Orlando, R. Dovesi. J. Comput. Chem. 29, 1450 (2008).

- [44] R.A. Jackson, E.M. Maddoc, M.E.G. Valerio. IOP Conf. Ser. Mater. Sci. Eng. 15, 012014 (2010)
- [45] J. Dabachi, M. Body, J. Dittmer, A. Rakhmatullin, F. Fayon, C. Legein. Dalton Trans., 48, 587 (2019).
- [46] P. Loiko, J.-L. Doualan, L. Guillemot, R. Moncorge, F. Starecki, A. Benayad, E. Dununa, A. Kornienko, L. Fimocheva, A. Braud, P. Camy, J. Lumin. 225, 117279 (2020).
- [47] A. Togo. Ab-initio phonon calculations for KY₃F₁₀/Fm-3m(225) // materials id.2943.
- [48] A. Togo. J. Phys. Soc. Jpn. 92, 012001 (2023).

Translated by M.Verenikina